Carbon stable isotopes as a palaeoclimate proxy in vascular plant dominated peatlands

M.J. Amesbury [a,*], D.J. Charman [a], R.M. Newnham [b], N.J. Loader [c],
J.P. Goodrich [d], J. Royles [e], D.I. Campbell [d], T.P. Roland [a], A. Gallego-Sala [a]

[a] *Geography, College of Life and Environmental Sciences, University of Exeter, Exeter, UK*
[b] *School of Geography, Earth and Environmental Sciences, Victoria University of Wellington, Wellington, New Zealand*
[c] *Department of Geography, College of Science, Swansea University, Swansea, UK*
[d] *School of Science, University of Waikato, Hamilton, New Zealand*
[e] *Department of Plant Sciences, University of Cambridge, Cambridge, UK*

Received 20 October 2014; accepted in revised form 4 May 2015; available online 12 May 2015

Abstract

Carbon stable isotope ($\delta^{13}C$) records from vascular plant dominated peatlands have been used as a palaeoclimate proxy, but a better empirical understanding of fractionation processes in these ecosystems is required. Here, we test the potential of $\delta^{13}C$ analysis of ombrotrophic restiad peatlands in New Zealand, dominated by the wire rush (*Empodisma* spp.), to provide a methodology for developing palaeoclimatic records. We took surface plant samples alongside measurements of water table depth and (micro)climate over spatial (six sites spanning > 10° latitude) and temporal (monthly measurements over 1 year) gradients and analysed the relationships between cellulose $\delta^{13}C$ values and environmental parameters. We found strong, significant negative correlations between $\delta^{13}C$ and temperature, photosynthetically active radiation and growing degree days above 0 °C. No significant relationships were observed between $\delta^{13}C$ and precipitation, relative humidity, soil moisture or water table depth, suggesting no growing season water limitation and a decoupling of the expected link between $\delta^{13}C$ in vascular plants and hydrological variables. $\delta^{13}C$ of *Empodisma* spp. roots may therefore provide a valuable temperature proxy in a climatically sensitive region, but further physiological and sub-fossil calibration studies are required to fully understand the observed signal.
© 2015 The Authors. Published by Elsevier Ltd. This is an open access article under the CC BY license (http://creativecommons.org/licenses/by/4.0/).

1. INTRODUCTION

Ombrotrophic peatlands provide potential sources of carbon stable isotope ($\delta^{13}C$) derived palaeoclimate data in many regions of the world, but exploitation of this record has been mostly limited to Northern Hemisphere *Sphagnum* moss dominated bogs (e.g. Price et al., 1997; Loisel et al., 2009, 2010; Moschen et al., 2009; Kaislahti-Tillman et al., 2010) with limited application in the Southern Hemisphere (Broder et al., 2012; Royles et al., 2012). In *Sphagnum* dominated peatlands, $\delta^{13}C$ has been primarily interpreted as a palaeohydrological proxy due to the correlation of *Sphagnum* cellulose $\delta^{13}C$ with both surface moisture gradients (Price et al., 1997; Ménot and Burns, 2001; Ménot-Combes et al., 2004; Loisel et al., 2009) and other palaeohydrological proxies in fossil studies (Lamentowicz et al., 2008; Loisel et al., 2010; van der Knapp et al., 2011). However, these relationships are not consistently reported (Markel et al., 2010) and empirical relationships have also been determined between *Sphagnum* $\delta^{13}C$ and temperature (Skrzypek et al., 2007; Holzkämper et al., 2012), which have subsequently been

* Corresponding author. Tel.: +44 (0)1392 725892.
  E-mail address: m.j.amesbury@exeter.ac.uk (M.J. Amesbury).

applied to fossil material to produce temperature reconstructions (Moschen et al., 2011).

Peatlands dominated by vascular plants are particularly common in low latitudes and the Southern Hemisphere, both regions where there are still relatively few high resolution Holocene palaeoclimate records. Such sites offer potential for stable isotope derived palaeoclimate records. $\delta^{13}C$ time series have, for example, been developed from bulk peat cellulose (Hong et al., 2001, 2005, 2010; Ma et al., 2008; Zhang et al., 2011) or a combination of bulk and single-species cellulose (Hong et al., 2003) from Chinese herbaceous peatlands. These were interpreted as a proxy for precipitation or humidity based on the correlation of $\delta^{13}C$ in modern herbaceous plant samples with annual precipitation values over broad spatial scales (Wang et al., 2003; Zhang et al., 2003; Liu et al., 2005). Conversely to studies in *Sphagnum* peatlands, no significant relationship between $\delta^{13}C$ and temperature was identified in these sites/regions. However, physiologically, temperature may affect stable carbon isotopic fractionation in vascular plants (Farquhar et al., 1989), including both potential direct (e.g. biochemical temperature dependence of Rubisco fractionation; Ménot and Burns, 2001) or indirect effects (e.g. on plant metabolism, for example, higher temperatures leading to increased assimilation rate, reduced discrimination against $^{13}CO_2$ and more heavy isotope enriched $\delta^{13}C$ values i.e. a positive relationship between $\delta^{13}C$ and temperature).

During photosynthesis, stable carbon isotopic fractionation occurs during the diffusion of atmospheric CO_2 to chloroplasts and during assimilation of inorganic carbon into plant tissues (O'Leary, 1981; Farquhar et al., 1989). For plants using the C3 photosynthetic pathway, the primary enzymatic fractionation occurs via Rubisco, which strongly discriminates against $^{13}CO_2$ (approximately 27‰). Models have been developed that describe stable carbon isotopic fractionation including these and other processes (Farquhar et al., 1989; White et al., 1994). Differences exist between models for vascular and non-vascular plants (Figge and White, 1995), largely to account for the presence/absence of stomata and subsequent consequences for CO_2 diffusion. For example, the constant used for fractionation occurring due to CO_2 diffusion through the boundary layer for mosses (2.9‰) is different to that for fractionation due to stomatal resistance in vascular plants (4.4‰). Diffusion limitation at the boundary layer is primarily governed by light, temperature and water availability, whereas diffusion limitation by stomatal resistance is primarily governed by relative humidity (White et al., 1994).

In photosynthetically active vascular plants, the physiological effect of an increase in humidity is an increase in stomatal conductance and therefore a decrease in $\delta^{13}C$ (i.e. more ^{13}C depleted or more negative $\delta^{13}C$ values; see Eq. 2, Ménot and Burns, 2001, p. 234). Conversely, when humidity is low, a large leaf to air vapour pressure deficit (VPD) exists between the saturated sub-stomatal cavity and the relatively dry atmosphere. This results in closing of stomata to reduce the rate of passive water loss, which in turn also reduces the rate of inward CO_2 diffusion and leads to a pool of CO_2 inside the leaf which experiences reduced interaction with atmospheric CO_2. This pool becomes progressively enriched in ^{13}C as the plant continues to assimilate carbon and the ratio of intercellular to atmospheric CO_2 concentration (C_i/C_a) drops, resulting in more positive $\delta^{13}C$ values (Figge and White, 1995).

Water availability *per se* should have less effect on vascular plants than non-vascular plants due to the ability of vascular plants to regulate water uptake and loss via stomatal conductance and to develop deep and/or extensive root systems which enable them to avoid becoming water-stressed during the summer water table deficit period that characterises peat forming regions (Ménot and Burns, 2001). Instead, stomatal constraints on CO_2 assimilation and their effect on photosynthetic water use efficiency (i.e. the ratio of carbon assimilated to water transpired by plants; Seibt et al., 2008), mediated by water supply, are the dominant control of stable carbon isotopic fractionation in vascular plants, at least over large spatial scales (Diefendorf et al., 2010).

Given the variability in the expected (i.e. from physiological models and understanding of fractionation processes) and observed (in both modern and fossil studies) relationships between $\delta^{13}C$ and climatic variables in both *Sphagnum* and vascular plant dominated peatlands, it is crucial that palaeoclimatic interpretations of $\delta^{13}C$ are empirically and mechanistically grounded and calibrated with modern climate data (Ménot and Burns, 2001; Stebich et al., 2011). Furthermore, because different chemical compounds and plant species record significantly different isotopic ratios (Ménot and Burns, 2001; Pancost et al., 2003; Moschen et al., 2009; Nichols et al., 2010; Stebich et al., 2011), both calibration and fossil studies need to use a common compound, typically α-cellulose prepared from a single taxon (Loader et al., 1997). *Sphagnum* provides a suitable substrate for stable isotopic analysis in many Northern Hemisphere peatlands, but is absent or less common in other parts of the world. In New Zealand, ombrotrophic peatlands are often almost entirely dominated by *Empodisma* spp. (Whinam and Hope, 2005; Clarkson and Clarkson, 2006; McGlone, 2009; Hodges and Rapson, 2010), recently classified into the two species *Empodisma minus* and *Empodisma robustum* (Wagstaff and Clarkson, 2012). These species are the primary Holocene peat former in New Zealand and occur separately north and south of the 'Kauri Line' at approximately 38° S (Fig. 1), forming predominantly monospecific peat deposits. *E. minus* and *E. robustum* are ecologically similar and distinguished by their growth forms and regeneration strategies following fire disturbance (Wagstaff and Clarkson, 2012). Both species have reduced, scale-like leaves on narrow stems, high water-use efficiency, root clusters with similar base exchange and water holding capacities to *Sphagnum*, can reduce water loss by controlling stomatal opening and form a dense canopy of living and dead shoots that protect the water-retaining matrix of cluster roots at the bog surface (Agnew et al., 1993; Clarkson et al., 2004; Wagstaff and Clarkson, 2012). Partly as a result of this dense vegetative canopy, surface evaporation rates are approximately half those reported for other wetlands dominated by vascular plants (Campbell and Williamson, 1997).
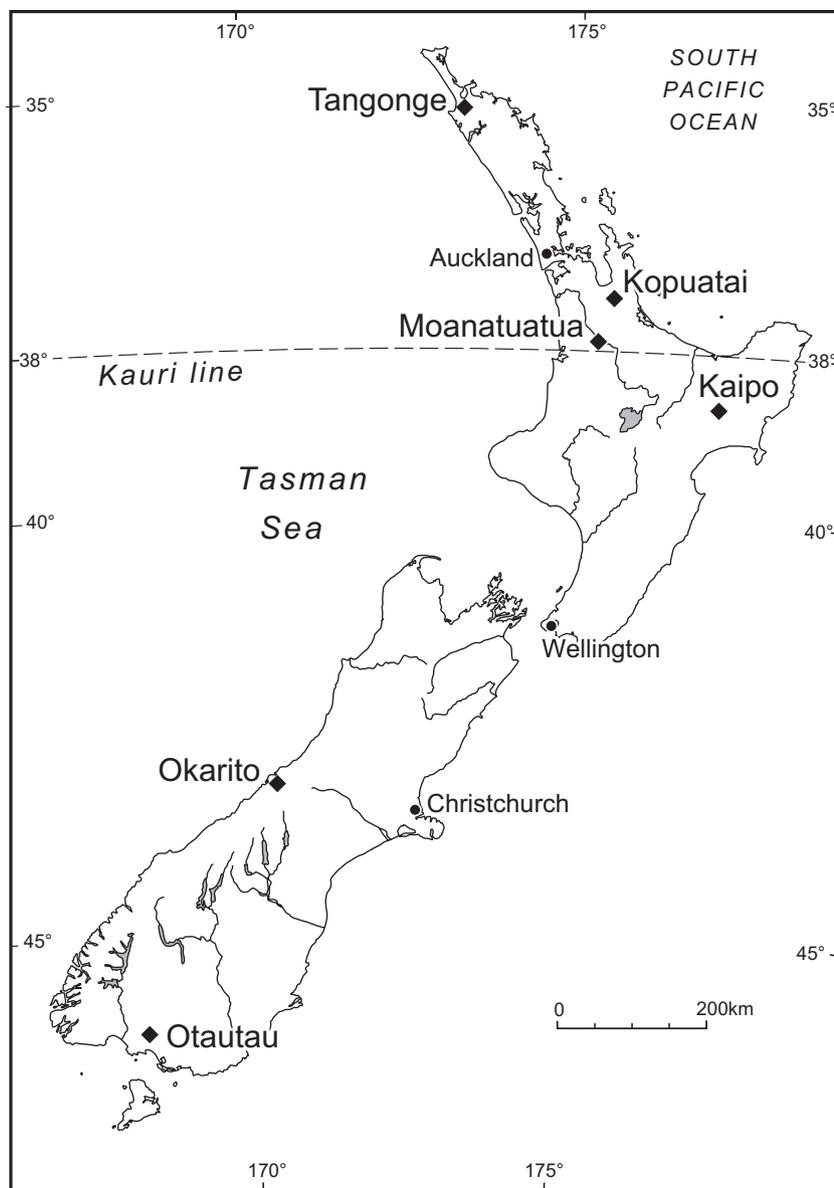
Fig. 1. Site locations. Kauri line represents the geographical split in the distribution of the two *Empodisma* species *E. robustum* (to the north of 38°) and *E. minus* (to the south of 38°).

The preserved remains of the surface cluster root matrix form deep peat deposits of full Holocene age in locations throughout New Zealand (e.g. Newnham et al., 1995, 2007; Newnham and Lowe, 2000; Vandergoes et al., 2005). *Empodisma* dominated ombrotrophic bogs therefore provide an ideal location to undertake empirical research to better understand carbon isotope fractionation in vascular peatlands because they are well suited to single-taxon analysis across broad climatic gradients in the climatically sensitive Southern Hemisphere mid-latitudes (e.g. Alloway et al., 2007; Lorrey et al., 2007; Ummenhofer and England, 2007; Fletcher and Moreno, 2012). These bogs also preserve potentially decadal-multidecadal resolution full Holocene records that offer the opportunity for stable carbon isotope based palaeoclimate reconstructions where

other suitable proxies are currently lacking. We therefore aim to test the ability of $\delta^{13}C$ analysis of ombrotrophic restiad peatlands in New Zealand to provide a methodology for developing palaeoclimatic records.

2. METHODS

2.1. Sites and field sampling

Six *Empodisma* dominated peatlands were selected to span climate gradients across New Zealand (Fig. 1; Table 1). The three northern sites, Tangonge (TNG), Kopuatai (KOP) and Moanatuatua (MOA) are dominated by *E. robustum* whereas the three sites south of the Kauri Line, Kaipo (KAI), Okarito (OKA) and Otautau (OTT),

Table 1
Site data. Water table depth values are as measured at time of sampling. Climate data were downloaded from the NIWA Virtual Climate Station Network (including the soil moisture index) and extracted from Kaplan et al. (2003), see Section 2.1. GDD0 = growing degree days above 0 °C.

Site	Region	Lat (°S)	Long (°E)	Altitude (m)	Empodisma species	WTD range (min–max, cm)	WTD mean (cm)	Temperature (°C)		Precipitation (mm)		Relative humidity (%)	Soil moisture index (mm)	GDD0 (°C)	PAR0 (mol photons m^{-2} season^{-1})	Total summer P-E deficit (mm)
								Mean annual	Mean summer	Total annual	Total summer					
TNG	Northland	35.1048	173.2156	10	E. robustum	7 (27–34)	30.5	15.85	19.21	1318	259	84.9	−57.5	5770	10,058	216
KOP	Waikato	37.3879	175.5552	5	E. robustum	8 (4–12)	8.3	14.72	19.05	1186	242	80.5	−60.6	5356	9739	181
MOA	Waikato	37.9235	175.3701	60	E. robustum	23 (50–73)	59.7	13.63	18.04	1186	256	82.8	−55	4960	9616	132
KAI	Te Urewera National Park	38.6849	177.2011	1000	E. minus	24 (5–29)	19.3	9.96	14.70	2665	521	82.4	−25	3641	8905	0
OKA	West Coast	43.2471	170.2205	75	E. minus	16 (−5*–11)	2.5	11.72	15.19	3338	887	84.3	−7.6	4277	9282	0
OTT	Southland	46.1311	168.0324	65	E. minus	14 (3–17)	7.5	9.98	14.09	1053	276	82.8	−40	3627	8506	114

* Minimum value of −5 cm for Okarito indicates that cluster roots were 5 cm below the standing water table at the bog surface.

are dominated by *E. minus* (Wagstaff and Clarkson, 2012). We employed both spatial and temporal approaches to sampling and analysis. For the spatial approach, we sampled 6 locations on each site in November 2012, providing a total dataset of 36 sampling points. At each sampling point, we took two plant samples (surface roots and recent shoot growth) and a water table depth measurement. Climate data for mean annual and summer (DJF) temperature, total annual and summer precipitation, relative humidity, soil moisture and potential evaporation were downloaded from the New Zealand National Institute for Water and Atmospheric Research (NIWA) National Climate Database (cliflo.niwa.co.nz). The 0.05° × 0.05° gridded Virtual Climate Station Network data points containing each of our sites were used to calculate long term annual averages (or sums for precipitation) from 1972 to 2013. These data were used to calculate growing degree days above 0 °C (GDD0; growing season warmth expressed as accumulated temperature over the growing season) and total summer precipitation minus potential evaporation (Supplementary Fig. 1). Cumulative photosynthetically active radiation over the growing season (above 0 °C, PAR0) was calculated from the relevant 0.5° × 0.5° grid square of the CLIMATE2.2 dataset of Kaplan et al. (2003), because the NIWA data did not contain cloudiness, which is required to calculate PAR0 (Prentice et al., 1993).

To help understand seasonal changes, we took monthly samples of root and recent shoot growth samples at two locations on one site (KOP) from November 2012 to November 2013 to provide a temporal data set. Water table depth was recorded daily over the year using a pressure transducer (WL1000 W, Hydrological Services, NSW, Australia) 1.5 m below the surface within a perforated PVC dip-well, located within 100 m of the two sampling locations. Air temperature was measured at 4.25 m above the surface with a fully aspirated probe (HMP155, Vaisala, Helsinki, Finland) and precipitation was measured using a tipping bucket rain gauge (TB5, Hydrological Services, NSW, Australia) situated 0.8 m (mean canopy height) above the surface. Half-hourly means of water table depth and air temperature and half-hourly sums of precipitation were recorded by data loggers and daily (24 h) means (or sums for precipitation) were calculated for analysis. To provide comparative microclimatic data, we also installed two miniature temperature and relative humidity data loggers (iButton, Maxim Integrated, CA, USA) within the zone of the cluster root microclimate, below the vegetative cover of the shoots. These were programmed to take four-hourly measurements for one year from November 2012 to October 2013 and we calculated daily (24 h) means for analysis.

2.2. δ^{13}C analyses

Samples of root and shoot material were prepared to α-cellulose using a standard methodology (Loader et al., 1997; Daley et al., 2010). Shoots were cut into short (approximately 1 mm) sections prior to chemical treatment (bleaching). Roots were cleaned with distilled water and manually separated from other plant material. Each root

sample was wet-sieved to remove fine detritus and then placed in a petri dish under a low powered microscope at ×10 magnification to remove all other plant remains until the sample comprised pure *Empodisma* cluster rootlets. These were also cut into short sections before bleaching. Five one hour bleaching stages were sufficient to form white cellulose samples for the root material (Daley et al., 2010), but up to 10 one hour bleaching stages were required for shoot samples to obtain a product of similar visual purity. 300–350 mg of prepared α-cellulose was weighed (in triplicate) into silver foil capsules, lightly crimped and pyrolised to carbon monoxide (CO) over glassy carbon in a flow of helium at 1400 °C (Young et al., 2011; Woodley et al., 2012). Stable carbon isotope ratios ($\delta^{13}C$) were reported as per mil (‰) deviations from the VPDB standard (where $\delta^{13}C$ (‰) $= (R_{sample}/R_{standard}) - 1$, where R is the ratio of $^{13}C/^{12}C$ in the sample and standard). A mean of three isotope measurements was calculated for each sample. Mean analytical precision on the replicate measurements method was 0.08‰ (σ_{n-1} $n = 44$ means comprising 131 individual measurements), which compares favourably with 0.1–0.12‰ (σ_{n-1} $n > 900$) reported elsewhere for $\delta^{13}C$ measured by both pyrolysis and combustion (Woodley et al., 2012; Young et al., 2012; Loader et al., 2013).

2.3. Stomatal density

Stomatal density (per mm^{-2}) was calculated using the impression technique (e.g. Sekiya and Yano, 2008; Xu and Zhou, 2008) for shoot samples at the northernmost (TNG) and southernmost (OTT) sites on the climate gradient to test whether stomatal density differed between species. At each site, shoots from three different sampling locations were used. For each sampling location, the central section of three individual shoots were selected, cut into short (approximately 5 cm) sections and painted with clear nail varnish. After approximately 30 min, the dried nail varnish was carefully removed and three replicate sections from each shoot were photographed at ×200 magnification (photo size was 450 × 335 μm, 0.15 mm^{-2}), resulting in 27 images per site from which to calculate mean stomatal density values.

3. RESULTS

Full $\delta^{13}C$ and water table depth results for the spatial and temporal datasets are shown in Supplementary Tables 1 and 2. Mean $\delta^{13}C$ values for *Empodisma* roots

and shoots in both the spatial and temporal datasets conform to the expected values for plants using the C3 photosynthetic pathway (Table 2; Farquhar et al., 1989). The limited microtopographical variability evident on the surface of *Empodisma* dominated restiad peatlands is reflected in the narrower range of $\delta^{13}C$ values compared to studies in *Sphagnum* dominated peatlands (approximately 6‰ range between hummocks and hollows; Price et al., 1997; Loisel et al., 2009). In the spatial samples, the predominant source of variability in water table depth was between, rather than within, sites and in part reflected the overall condition and management status of the sites. MOA was the driest site, with its minimum value for water table depth exceeding the maximum values at all other sites (Table 1). The two driest sites, MOA (mean water table depth of 59.7 cm) and TNG (mean water table depth of 30.5 cm) are remnants of previously far more extensive peatlands surrounded by drained agricultural land which has affected the local hydrological regime, whereas the other sites are more extensive and pristine and function more independently as hydrological units with correspondingly shallower water tables (KOP 8.3 cm; KAI 19.3 cm; OKA 2.5 cm; OTT 7.5 cm).

Climate parameters show clear gradients across the site transect (Table 1). Temperature (mean annual and summer) declines with increasing latitude, also reflected in the values of GDD0 and PAR0, which show that conditions for photosynthesis are generally better in the North Island sites. The exception to these trends is KAI, which has lower temperature, GDD0 and PAR0 values compared to the other North Island sites as a result of its higher altitude. Precipitation patterns in New Zealand are strongly influenced by regional circulation patterns and climate modes with a strong orographic effect (Kidson, 2000; Lorrey et al., 2007; Ummenhofer and England, 2007). This is reflected in the mean annual and summer precipitation values. KOP, MOA and OTT have similar annual values with OTT receiving proportionally more rain during summer. TNG has higher annual precipitation but summer precipitation is similar to KOP and MOA. Values for both annual and summer precipitation are higher at KAI due to its higher elevation, and at OKA, due to its location west of the Southern Alps in the path of the prevailing southern westerlies. Higher precipitation values mean there is no summer P-E deficit period at these sites, whereas the remaining four sites (TNG, KOP, MOA and OTT) all experience a deficit during the summer that could result in a drawdown of water table. The overall duration and severity

Table 2
Range in $\delta^{13}C$ and water table depth measurements is correspondingly higher in the spatial samples compared to the temporal samples.

	Mean $\delta^{13}C$ all samples (‰)	Range in $\delta^{13}C$ values (‰)	Mean all WTD values (cm)	Range in WTD values (min–max) (cm)
Spatial roots	−25.57	2.8	21.3	78 (−5[*]–73)
Spatial shoots	−24.72	3.77		
Temporal roots	−25.70	1.15	10.5	23.6 (1.6–25.1)
Temporal shoots	−24.51	1.23		

[*] Minimum value of −5 cm for Okarito indicates that cluster roots were 5 cm below the standing water table at the bog surface.

of this period is strongly linked to latitude with TNG experiencing the longest and most severe and OTT the shortest and least severe deficit (Table 1, Supplementary Fig. 1).

3.1. Spatial samples

Correlations between mean site $\delta^{13}C$ values of roots and shoots at each site with regional climate data indicate significant relationships with broad climate gradients (Fig. 2; Table 3). Annual and summer temperatures are significantly negatively correlated with $\delta^{13}C$, suggesting that as temperature increases, *Empodisma* cellulose becomes more ^{13}C depleted (Fig. 2A). The same relationships are evident

with PAR0 and GDD0 suggesting that higher PAR and growing season warmth results in more negative $\delta^{13}C$ values (Fig. 2C and D). The correlation between PAR0 and GDD0 is high ($r = 0.99$, $p \leqslant 0.0001$) as both variables include growing season length (Charman et al., 2013), so the consistent relationships observed between these climate parameters and $\delta^{13}C$ should be expected. There were no significant relationships with total annual or summer precipitation, relative humidity or soil moisture (Fig. 2B, E, F, Table 3). Taking the variables highlighted as significant in Table 3, R v. 3.0.2 (R Development Core Team, 2014) was then used to build multivariate linear models by stepwise linear regression (using the Akaike Information
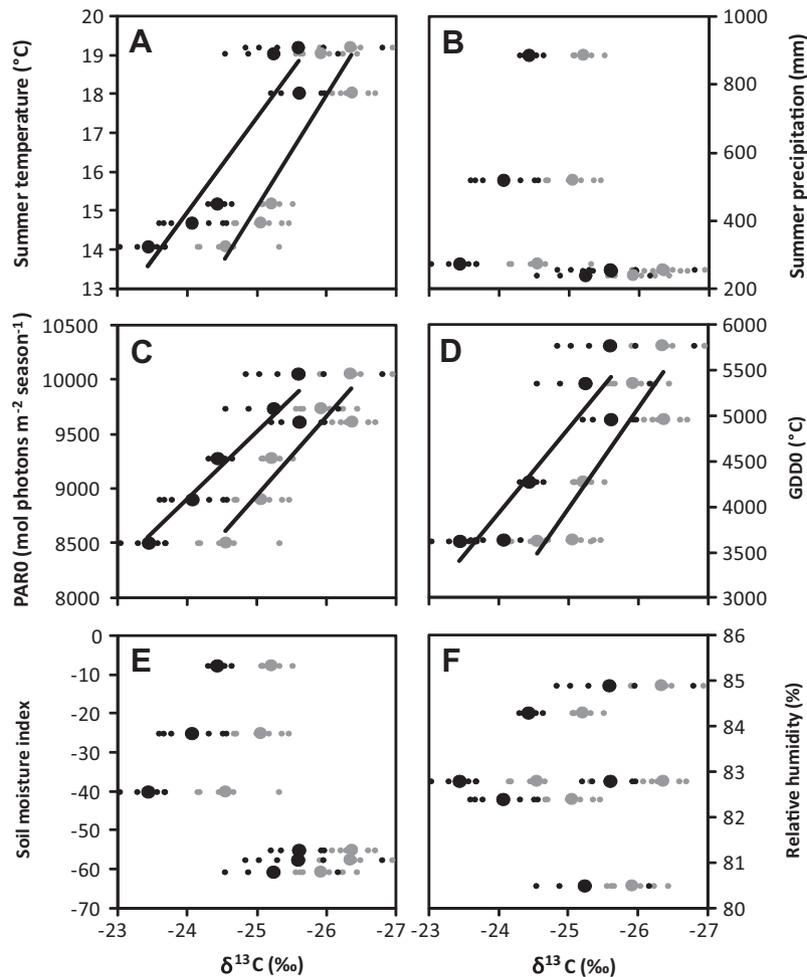

Fig. 2. Correlations between root (grey circles) and shoot (black circles) $\delta^{13}C$ (‰) and indicators of broad climate gradients over the spatial dataset. Large symbols are an average of the six within site data points shown as small grey/black symbols. See Table 5 for r and p values corresponding to these data.

Table 3
Correlation coefficients between root and shoot $\delta^{13}C$ and indicators of broad climate gradients over the spatial dataset. Climate data as per Table 1. Significant results given in bold with p values < 0.1 in parentheses.

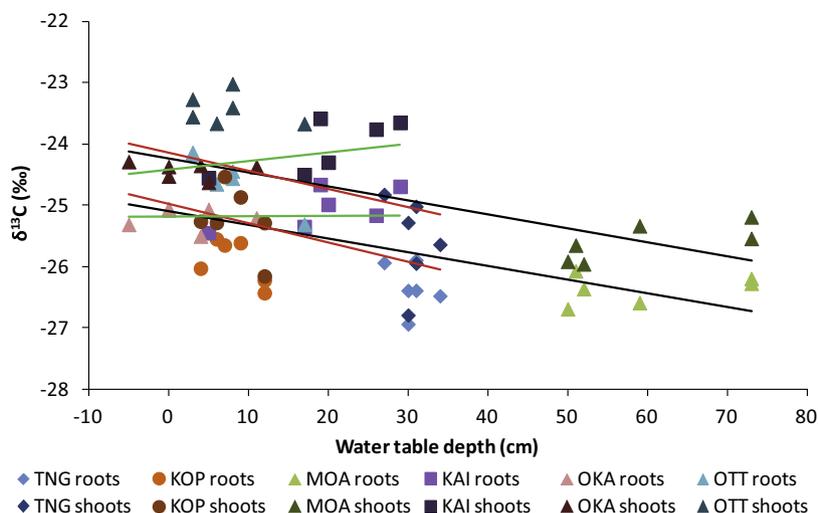|	Annual temperature	Summer temperature	Annual precipitation	Summer precipitation	Relative humidity	Soil moisture	PAR0	GDD0
Roots	**−0.91 (0.012)**	**−0.93 (0.006)**	0.36	0.41	−0.08	0.66	**−0.94 (0.005)**	**−0.91 (0.012)**
Shoots	**−0.92 (0.009)**	**−0.94 (0.005)**	0.31	0.34	−0.07	0.62	**−0.96 (0.002)**	**−0.92 (0.009)**

Fig. 3. $\delta^{13}C$ (‰) against water-table depth for spatial root and shoot cellulose samples, sub-divided by site. Linear trendlines are shown for the full (black), without MOA (red) and pristine only (green) datasets. In all cases, the lower trendline is for root samples and the upper trendline for shoot samples. Strength, direction and significance of these relationships are given in Table 3.

Criterion to choose the most parsimonious model) for both roots and shoots. The inter-correlation of summer and mean annual temperature meant they could not be used as independent variables and therefore summer temperature was omitted. The variation of $\delta^{13}C$ of root cellulose was best described by a linear model with an adjusted R^2 of 0.78 ($p < 0.001$) including PAR0 ($p < 0.001$), mean annual temperature ($p = 0.004$), and GDD0 ($p = 0.004$). Similarly, variation in $\delta^{13}C$ of shoot cellulose was best described by a linear model with an adjusted R^2 of 0.77 ($p < 0.001$) including PAR0 ($p = 0.001$), GDD0 ($p = 0.01$) and mean annual temperature ($p = 0.01$). Testing the significance of the relationships of temperature, PAR0 and GDD0 with $\delta^{13}C$ in a multivariate framework mitigated against potential Type-2 errors and provided greater confidence in the analysis of the observed results.

We also tested the relationship between $\delta^{13}C$ values and water table to examine the potential effect of water availability on $\delta^{13}C$, which has been observed in other studies. Increased water stress would be expected to lead to ^{13}C enriched cellulose such that water table depth should be positively correlated with $\delta^{13}C$ (White et al., 1994; Ménot

and Burns, 2001). When the full spatial dataset is considered, $\delta^{13}C$ of both root and shoot material is significantly negatively correlated to water table depth (Fig. 3; Table 4) with more negative $\delta^{13}C$ values associated with deeper water tables/drier conditions and more positive (i.e. less negative) $\delta^{13}C$ values with shallower water tables/wetter conditions. However, closer inspection of the data shows this relationship is driven by the two extreme dry sites of MOA and TNG, where water tables have been artificially lowered. When these were removed, there was no significant relationship between the $\delta^{13}C$ of either roots or shoots and water table depth (Fig. 3; Table 4). The relationship present for the whole data set is thus more likely related to the fact that the two driest sites are both situated in relatively warm climatic settings. Their low $\delta^{13}C$ values are more likely to be driven by temperature and related variables (Fig. 2) than by moisture availability.

We measured stomatal density in shoot samples from the northernmost (TNG) and southernmost (OTT) sites to examine the potential for physiological adaptations that may explain the observed relationships between $\delta^{13}C$ and climate parameters. Mean values, based on 27 replicate measurements per site were 481 ± 51 (one standard deviation) stomata mm^{-2} at TNG and 508 ± 111 stomata mm^{-2} at OTT. A two sample t-test showed no significant difference between the two sites ($p = 0.259$, df = 26).

3.2. Temporal samples (Kopuatai)

There was much lower variability in water table depth measured in the temporal samples over a 1 year period as compared to the spatial samples collected over climate gradients (Tables 1 and 2). The range in water table depth in the spatial samples was 78 cm compared to 23.6 cm for the temporal samples. The ranges of $\delta^{13}C$ values for both roots and shoots were also lower (Table 2).

Table 4
Correlations and significance of root and shoot cellulose $\delta^{13}C$ (‰) with water table depth for complete spatial dataset ('All', $n = 36$), a subset excluding MOA ('Without MOA', $n = 30$) and a subset including only the pristine sites, which excludes TNG and MOA ('Pristine only', $n = 24$).

	Dataset	r	p
Root $\delta^{13}C$–WTD	All	−0.608	<0.01
Shoot $\delta^{13}C$–WTD	All	−0.513	<0.05
Root $\delta^{13}C$–WTD	Without MOA	−0.492	<0.05
Shoot $\delta^{13}C$–WTD	Without MOA	−0.373	<0.05
Root $\delta^{13}C$–WTD	Pristine only	0.010	0.964
Shoot $\delta^{13}C$–WTD	Pristine only	0.157	0.465

When plotted against water table depth (Fig. 4) both root and shoot δ^{13}C values showed relatively consistent values of around $-24\text{\textperthousand}$ and $-25\text{\textperthousand}$ respectively, regardless of fluctuations in water table depth over the annual cycle. These values are consistent with the KOP results from the spatial dataset (Fig. 4), which spanned a narrower range of water table depth values but also did not show a clear relationship with water table depth. When plotted against sampling date (Fig. 5) with water table depth fluctuations over the year, some effect of water table is evident, with shoot samples becoming gradually more ^{13}C enriched from November to March as the bog became drier and water table depth increased over the summer. As the site became wetter and water table depth gradually decreased from April to June as precipitation increased, shoot δ^{13}C became more depleted. This is consistent with the direction of relationship that would be expected based on physiological understanding of carbon isotope fractionation in vascular plants by changes in stomatal conductance in response to relative humidity (Figge and White, 1995), but the minor and short term nature of the changes suggests that this is unlikely to have a significant impact on the average δ^{13}C signal of shoots over the entire year.

In comparison, root δ^{13}C showed relatively little variation over the year (Fig. 5), probably because the monthly root samples would likely reflect the integrated growth over a longer period of time than the shoot samples, where it was possible to ensure that only recent growth was sampled.
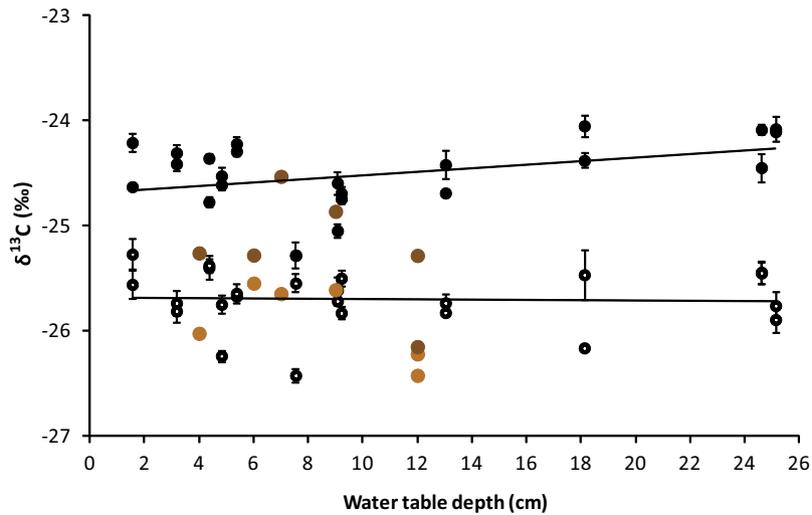

Fig. 4. δ^{13}C (‰) against water-table depth for Kopuatai temporal root (open circles) and shoot (closed circles) cellulose samples over the 12 months of sampling. Error is one standard deviation derived from three replicate measurements. Spatial dataset from the same site is included for comparison (roots = light orange circles; shoots = dark orange circles).
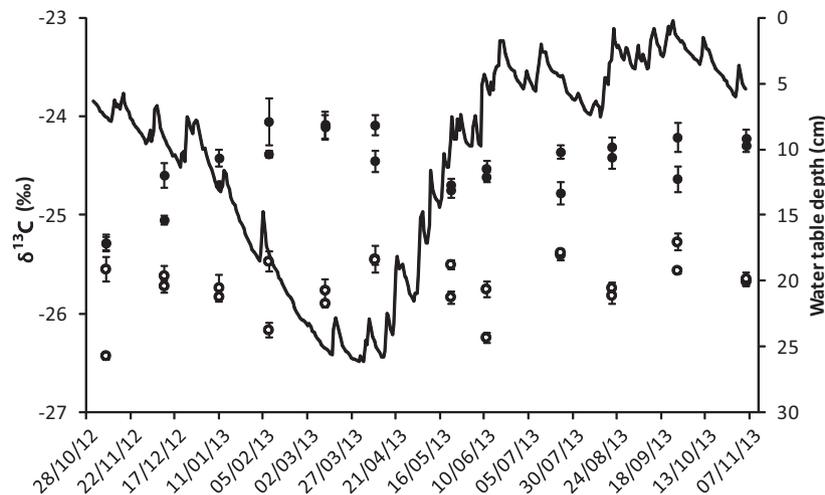

Fig. 5. δ^{13}C (‰) of Kopuatai temporal root (open circles) and shoot (closed circles) samples against sampling date with measured water table depth (black line) over the 12 months of sampling. Error margin is one standard deviation derived from three replicate measurements.

Because root and shoot samples taken on any given day represent the growth over a preceding period, temporal root and shoot $\delta^{13}C$ were also compared with mean water table depth over the preceding week, 2 weeks and 1 month, in addition to mean temperature and humidity recorded by the iButton data logger on the day of sampling (Tables 5 and 6). The strongest significant relationship was between shoot $\delta^{13}C$ and water table averaged over the 2 weeks prior to sampling ($r = 0.403$, $p = 0.051$). This weak positive correlation supports the contention of a minor but observable impact of summer water table draw down on shoot $\delta^{13}C$. Comparison of the iButton temperature data to air temperature and temperature measured using fine thermocouples attached to *E. minus* stems in the upper canopy (not shown) suggested that iButton temperature may have been slightly affected by heating from solar radiation but was a reasonable measure of temperature within the upper, live part of the canopy.

3.3. Root and shoot $\delta^{13}C$ offset and species specificity

Shoot cellulose was consistently more ^{13}C enriched than root cellulose for both the spatial and temporal datasets (Table 7) and there was a significant difference in the $\delta^{13}C$ values between *E. robustum* (TNG, KOP, MOA) and *E. minus* (KAI, OKA, OTT) dominated sites for both root and shoot cellulose (two tail, two sample *t*-test: $p \leqslant 0.0001$, df $= 17$). Our results show more negative mean $\delta^{13}C$ values associated with *E. robustum* dominated sites for both root and shoot cellulose and a broadly higher offset

between mean root and shoot values in *E. minus* sites (Table 7).

4. DISCUSSION

4.1. $\delta^{13}C$ and temperature

The significant and robust negative relationships observed with temperature, PAR0 and GDD0 provide a strong indication that *Empodisma* $\delta^{13}C$ is driven by climate parameters linked to growing season conditions, as opposed to those related to broad-scale (e.g. precipitation, soil moisture, relative humidity) or site-specific (e.g. water table depth) hydrology. Ménot and Burns (2001) reviewed the extent to which factors such as temperature and light intensity can affect $\delta^{13}C$ over climate gradients in both vascular plants and mosses. Field and laboratory studies show conflicting results for the influence of temperature on $\delta^{13}C$, with both positive (field studies only) and negative correlations (field and laboratory studies). In particular, Ménot and Burns (2001) and Skrzypek et al. (2007) found negative correlations between both vascular plant and moss $\delta^{13}C$ and temperature across altitudinal gradients of peat bogs in Switzerland and Poland respectively, with more enriched $\delta^{13}C$ as temperature decreased, which is consistent with our results. Theoretically, higher temperatures may be expected to increase assimilation rate, reducing discrimination against $^{13}CO_2$ and leading to more enriched $\delta^{13}C$ values, i.e. a positive relationship between $\delta^{13}C$ and temperature. However, carbon isotope fractionation in vascular plants

Table 5
Correlation coefficients (*r* values) between temporal root and shoot $\delta^{13}C$ (‰) at KOP, water table depth (WTD) metrics and microclimatic variables. Significant results given in bold with *p* values < 0.1 in parentheses.

	Root $\delta^{13}C$	Shoot $\delta^{13}C$	WTD on day	WTD previous week	WTD previous 2 weeks	WTD previous month	iButton temperature
Shoot $\delta^{13}C$	0.287						
WTD on day	0.043	**0.385** (0.063)					
WTD previous week	−0.026	0.309	**0.910** (<0.01)				
WTD previous 2 weeks	−0.062	**0.403** (0.051)	**0.971** (<0.01)	**0.928** (<0.01)			
WTD previous month	−0.020	0.333	**0.902** (<0.01)	**0.907** (<0.01)	**0.968** (<0.01)		
iButton temperature	−0.141	0.158	0.314	0.068	0.141	0.029	
iButton humidity	0.149	−0.237	**−0.665** (<0.01)	**−0.398** (0.066)	**−0.507** (0.016)	−0.354	**−0.853** (<0.01)

Table 6
Values for water table depth, climatic and microclimatic variables recorded over the 1 year (8/11/12–5/11/13) of sampling at Kopuatai, Waikato region. Water-table depth results are for sampling days only ($n = 12$). Air temperature and daily precipitation results are 24 h mean (temperature) and total (precipitation) values of 30 min frequency measurements over the full year (see Section 2.1). iButton results are from microclimatic data loggers placed at the peat surface, below the vegetative mass of *Empodisma* shoots, within the cluster root microclimate. Results are 24 h mean values of four hourly measurements from two iButtons from 19/11/12–5/11/13.

	Water-table depth (cm)	Air temperature (°C)	Daily precipitation (mm)	iButton temperature (°C)	iButton relative humidity (%)
Mean	10.5	13.8	2.7	14.0	90.2
Minimum	1.6	4.2	0	1.4	67.1
Maximum	25.1	22.5	47.7	25.6	100
Range	23.6	18.3	47.7	24.2	32.9

Table 7
Mean root and shoot cellulose $\delta^{13}C$ (‰) from spatial samples ($n = 6$ per site) and with offset between the two and its relation to *Empodisma* species.

Site	Mean root $\delta^{13}C$ ‰ (st. dev.)	Mean shoot $\delta^{13}C$ ‰ (st. dev.)	Root–shoot offset	*Empodisma* species
Tangonge	−26.33 (0.38)	−25.58 (0.72)	0.75	*E. robustum*
Kopuatai	−25.91 (0.36)	−25.23 (0.54)	0.68	*E. robustum*
Moanatuatua	−26.36 (0.24)	−25.60 (0.31)	0.76	*E. robustum*
Kaipo	−25.05 (0.33)	−24.06 (0.44)	0.99	*E. minus*
Okarito	−25.20 (0.18)	−24.42 (0.13)	0.78	*E. minus*
Otautau	−24.54 (0.43)	−23.43 (0.25)	1.11	*E. minus*

is governed by the balance between stomatal conductance and assimilation rate (White et al., 1994). Research at KOP has shown that *Empodisma* stomatal conductance is reduced, particularly on clear sunny days, in response to high VPD, partly causing very low observed rates of evapotranspiration (Campbell and Williamson, 1997). Air temperature and VPD are positively correlated and it has been hypothesised that as temperature and VPD increase beyond a photosynthetic optimum, assimilation rate declines, leading to a decrease in stomatal conductance in addition to the direct effect of VPD on stomatal conductance (Duursma et al., 2014). The effects of these interrelationships between assimilation rate and stomatal conductance in relation to temperature on $\delta^{13}C$ are unclear but underline the need for contemporary studies to provide the foundation for the interpretation of palaeo $\delta^{13}C$ records (See Table 8).

We propose several hypotheses that could lead to the observed negative relationships between $\delta^{13}C$ and temperature, PAR0 and GDD0 in this study. First, they could result only from the limitations of the space-for-time calibration approach. For example, confounding site effects may suggest environmental/climatic control when, in reality, other factors dominate inter-site variability to the extent that more physiologically acceptable relationships may be obscured. The differences between *E. robustum* and *E. minus* may be relevant here (see below) but we applied a robust statistical approach, meaning we can have confidence in the observed significant negative relationships, and we purposely selected sites spaced over a wide climatic gradient to minimise the likelihood that this would be a major influence (Section 3). Second, if growing conditions were consistently better at the northern sites, plants may have developed physiological adaptations over time, such as increased stomatal density, that would increase discrimination against $^{13}CO_2$ by increasing the supply of $^{12}CO_2$ given a constant assimilation rate. To test this we measured

stomatal density on shoot samples from the northernmost (TNG) and southernmost (OTT) sites, but results suggested that this hypothesis can be rejected. Third, the high density of *Empodisma* shoots coupled with generally wet, humid conditions may produce a boundary layer of water vapour through which diffusion of CO_2 is limited, as observed in astomatous bryophytes which have an external layer of capillary water (Rice and Giles, 1996; Williams and Flanagan, 1996). If temperature increased, relative humidity could drop, increasing the rate of diffusion to the leaf and consequently discrimination against $^{13}CO_2$. Year-round growing seasons have been observed at KOP (Goodrich et al., 2015) and MOA (Campbell et al., 2014). A longer growing season would result in a higher proportion of the seasonal assimilation occurring under more discriminating conditions, leading to more negative $\delta^{13}C$ values overall. Fourth, increased temperature could increase rates of microbial activity, which would increase the release of respiratory CO_2. Respiratory CO_2 is ^{13}C depleted compared to source (atmospheric) CO_2 (Ghashghaie et al., 2003; Bruggemann et al., 2011), so that an increased contribution of this as a source of CO_2 for carbon assimilation would lead to more negative $\delta^{13}C$ values at higher temperatures. Finally, Araya et al. (2010) identified significant differences in $\delta^{13}C$ of restionaceous species between male and female individuals. Although *Empodisma* was not included in their study, it is a dioecious species and it remains a possibility that the observed gradients in our data could be partly a result of a sex bias.

The processes by which the $\delta^{13}C$ signature in our sites is linked to temperature related climate parameters remain uncertain and further physiological research coupled with site monitoring is necessary to understand this. However, the strength and significance of the observed relationships suggest that *Empodisma* $\delta^{13}C$ may be a useful palaeoclimate proxy for temperature, PAR and growing season length. A test of these relationships could be undertaken

Table 8
Stomatal density (per mm^{-2}) results from TNG and OTT. Each result is the mean of three replicate counts, resulting in $n = 27$ individual measurements per site.

Site	Sample #	Shoot A	Shoot B	Shoot C	Site mean	Site standard deviation
Tangonge	1	491	511	491	481	55
Tangonge	2	489	493	518		
Tangonge	3	493	380	464		
Otautau	1	556	542	520	508	111
Otautau	2	473	420	407		
Otautau	3	424	656	578		

experimentally under controlled laboratory conditions and a further empirical test of the observed relationships over time could be undertaken by comparing $\delta^{13}C$ from dated fossil *Empodisma* to known instrumentally recorded climate events.

4.2. $\delta^{13}C$ and hydrology

Previous studies on $\delta^{13}C$ from both vascular plant and moss dominated peatlands have shown significant relationships to hydrological variables, but these are not found here. The lack of significant relationships between $\delta^{13}C$, precipitation and other hydrological factors (Table 3) supports the argument that *Empodisma* is not water-stressed, even during the summer P-E deficit period experienced at TNG, KOP, MOA and OTT during the summer months (Supplementary Fig. 1). The apparent significant negative correlation between water table depth and $\delta^{13}C$ in the full spatial dataset (Fig. 3) is predominantly driven by the extreme dryness of MOA and, to a lesser extent, TNG, both much drier due to the extensive drainage of surrounding land for agricultural use. Water table depth values for these sites appear to be largely outside of the range of naturally functioning restiad peatlands although at MOA it has been suggested that past water tables may also have been naturally lower due to the site's hydrological setting (Campbell et al., 2014). When MOA and TNG were removed from the dataset, there was no clear relationship between $\delta^{13}C$ and water table depth across the remaining pristine sites (Fig. 3; Table 4) and the range in sampled water table depths fell from 78 cm to 34 cm. This is more equivalent to the range of values recorded over the one year of sampling at KOP associated with the temporal dataset (26 cm).

There are a number of hypotheses that could explain the lack of relationship between water table depth and $\delta^{13}C$ in the spatial dataset of pristine sites (i.e. excluding MOA and TNG). First, the range of water table depths recorded may not have been wide enough to cause *Empodisma* to become water-stressed and therefore drive a relationship with $\delta^{13}C$, especially given its high water use efficiency (Wagstaff and Clarkson, 2012). The temporal dataset does show some response in shoot $\delta^{13}C$ over the summer months when water table depth dropped by *ca.* 20 cm, less than the range observed in the spatial dataset, suggesting there is some effect of water stress. However, this drawdown of water table took place during an historic drought from January to March 2013 (Goodrich et al., 2015) suggesting that this level of hydrological change may be an extreme case and supporting the previous contention that under more average climatic conditions, *Empodisma* is not water-stressed.

A second hypothesis is that the instantaneous sampling and water table measurements employed during data collection for the spatial dataset did not effectively capture the plant-hydrology relationship. This is possible because temporal $\delta^{13}C$ measurements on plant shoots showed the strongest relationship with water table depth when the average for the previous 2 weeks was taken. Physiological understanding of how water availability, primarily relative humidity in the case of vascular plants (White et al., 1994; Ménot and Burns, 2001), affects $\delta^{13}C$ is clear but reflects a theoretical, instantaneous situation. Conversely, $\delta^{13}C$ in organic matter will represent the assimilation weighted signal of a longer period of carbon assimilation, during which conditions for photosynthesis, driven by changes in moisture, temperature, light intensity or other environmental factors, may have varied. Sampling was undertaken during the growing season when a relationship between $\delta^{13}C$ and water table depth is most likely as conditions for photosynthesis are most favourable and significant changes in water table depth occur. However, Fig. 5 shows that at KOP, it is not until January, when water table depth begins to increase sharply, that there was a response in the $\delta^{13}C$ of new shoot growth. Over the rest of the annual cycle (Fig. 5) and in the spatial samples (Fig. 3), a clear response of root or shoot $\delta^{13}C$ is not evident suggesting that any relationship between $\delta^{13}C$ and surface moisture conditions is likely to be minor and restricted to the summer water deficit period, similar to biological proxies for water table (Charman, 2007).

4.3. Potential species effect

The significant differences between *E. robustum* and *E. minus* root and shoot cellulose $\delta^{13}C$ mean that some degree of the observed relationships between $\delta^{13}C$ and climate parameters may be caused by ecological or growth form differences between the two species, as opposed to broader scale climatic influences, though the split between the species is based on genetic rather than physiological research (Wagstaff and Clarkson, 2012). One potential explanatory mechanism relates to the higher density of the vegetative canopy of *E. robustum* (Wagstaff and Clarkson, 2012). In the upper canopy, where most living plant material is located, absolute humidity is generally well coupled to the atmosphere. However, relative humidity can be reduced because upper canopy temperature is often elevated due to limited plant transpiration and a higher sensible heat load. The denser canopy of *E. robustum* compared to *E. minus* could potentially lead to lower rates of evaporation from the peat surface, resulting in relatively higher air temperatures and lower relative humidity, leading to more positive $\delta^{13}C$ values. Conversely, a denser canopy could also reduce the mixing of atmospheric CO_2, leading to potential recycling of respiratory CO_2, which has a more depleted $\delta^{13}C$ signature (Ghashghaie et al., 2003; Bruggemann et al., 2011), and more negative $\delta^{13}C$ values at *E. robustum* sites. However, as the split between species is also strictly geographical (north and south of the 'Kauri Line' at 38°S; Wagstaff and Clarkson, 2012), we would expect that significant relationships to climate parameters over our site transect (Section 4.1) will also appear to result from a possible species effect. Without future physiological research into species differences, it is not currently possible to determine the extent to which either one of these influences predominates.

5. CONCLUSIONS

Ombrotrophic peatlands dominated by vascular plants are an important potential source of palaeoclimatic proxy

data in the form of $\delta^{13}C$ stable isotopic records, but an empirical framework for interpreting these records from fossil samples is lacking. We investigated the links between $\delta^{13}C$ in *Empodisma* roots and shoots on New Zealand peatlands and spatial and temporal variability in climate and hydrology. Our results suggest that the $\delta^{13}C$ signal in *Empodisma* dominated peatlands is influenced by differences in prevailing climate to a greater extent than site-specific differences in surface moisture, which is consistent with results from Chinese peatlands (e.g. Hong et al., 2001, 2010; Liu et al., 2005). We found the strongest relationships between $\delta^{13}C$ and temperature, PAR0 and GDD0. The lack of an observed relationship with hydrological variables can be explained by the absence of water stress for *Empodisma* at our sites. We conclude that $\delta^{13}C$ of *Empodisma* roots in New Zealand provides a new palaeoclimate proxy for temperature, but further physiological and fossil calibration studies are required to fully understand the observed climate–$\delta^{13}C$ relationships.

ACKNOWLEDGEMENTS

APPENDIX A. SUPPLEMENTARY DATA

Supplementary data associated with this article can be found, in the online version, at http://dx.doi.org/10.1016/j.gca.2015.05.011.

REFERENCES

Agnew A. D. Q., Rapson G. L., Sykes M. T. and Bastow Wilson J. (1993) The functional ecology of *Empodisma minus* (Hook. f.) Johnson & Cutler in New Zealand ombrotrophic mires. *New Phytol.* **124**, 703–710.

Alloway B. V., Lowe D. J., Barrell D. J. A., Newnham R. M., Almond P. C., Augustinus P. C., Bertler N. A. N., Carter L., Litchfield N. J., McGlone M. S., Shulmeister J., Vandergoes M. J. and Williams P. W.NZ-INTIMATE members (2007) Towards a climate event stratigraphy for New Zealand over the past 30,000 years. *J. Quat. Sci.* **22**, 9–35.

Araya Y. N., Silvertown J., Gowing D. J., McConway K., Linder P. and Midgley G. (2010) Variation in $\delta^{13}C$ among species and sexes in the family *Restionaceae* along a finescale hydrological gradient. *Austral Ecol.* **35**, 818–824.

Broder T., Blodau C., Biester H. and Knorr K. H. (2012) Peat decomposition records in three pristine ombrotrophic bogs in southern Patagonia. *Biogeosciences* **9**, 1479–1491.

Brüggemann N., Gessler A., Kayler Z., Keel S. G., Badeck F., Barthel M., Boeckx P., Buchmann N., Brugnoli E., Esperschütz J., Gavrichkova O., Ghashghaie J., Gomez-Casanovas N., Keitel C., Knohl A., Kuptz D., Palacio S., Salmon Y., Uchida Y. and Bahn M. (2011) Carbon allocation and carbon isotope fluxes in the plant-soil-atmosphere continuum: a review. *Biogeosciences* **8**, 3457–3489.

Campbell D. I. and Williamson J. L. (1997) Evaporation from a raised peat bog. *J. Hydrol.* **193**, 142–160.

Campbell D. I., Smith J., Goodrich J. P., Wall A. M. and Schipper L. A. (2014) Year-round growing conditions explains large CO_2 sink strength in a New Zealand raised peat bog. *Agric. Forest Meteorol.* **192–193**, 59–68.

Charman D. J. (2007) Summer water deficit variability controls on peatland water-table changes: implications for Holocene palaeoclimate reconstructions. *Holocene* **17**, 217–227.

Charman D. J., Beilman D. W., Blaauw M., Booth R. K., Brewer S., Chambers F. M., Christen J. A., Gallego-Sala A., Harrison S. P., Hughes P. D. M., Jackson S. T., Korhola A., Mauquoy D., Mitchell F. J. G., Prentice I. C., van Der Linden M., De Vleeschouwer F., Yu Z. C., Alm J., Bauer I. E., Corish Y. M. C., Garneau M., Hohl V., Huang Y., Karofeld E., Le Roux G., Loisel J., Moschen R., Nichols J. E., Nieminen T. M., MacDonald G. M., Phadtare N. R., Rausch N., Sillasoo Ü., Swindles G. T., Tuittila E. S., Ukonmaanaho L., Väliranta M., van Bellen S., van Geel B., Vitt D. H. and Zhao Y. (2013) Climate-related changes in peatland carbon accumulation during the last millennium. *Biogeosciences* **10**, 929–944.

Clarkson B. R. and Clarkson B. D. (2006) Restiad bogs in New Zealand. In *The Biology of Peatlands* (eds. H. Rydin and J. Jeglum). University of Oxford Press, Oxford, pp. 228–232.

Clarkson B. R., Schipper L. A. and Lehmann A. (2004) Vegetation and peat characteristics in the development of lowland restiad peat bogs, North Island, New Zealand. *Wetlands* **24**, 133–151.

Daley T. J., Barber K. E., Street-Perrott F. A., Loader N. J., Marshall J. D., Crowley S. F. and Fisher E. H. (2010) Holocene climate variability revealed by oxygen isotope analysis of *Sphagnum* cellulose from Walton Moss, northern England. *Quatern. Sci. Rev.* **29**, 1590–1601.

Diefendorf A. F., Mueller K. E., Wing S. L., Koch P. L. and Freeman K. H. (2010) Global patterns in leaf ^{13}C discrimination and implications for studies of past and future climate. *Proc. Nat. Acad. Sci.* **107**, 5738–5743.

Duursma R. A., Barton C. V. M., Lin Y.-S., Medlyn B. E., Eamus D., Tissue D. T., Ellsworth D. S. and McMurtie R. E. (2014) The peaked response of transpiration rate to vapour pressure deficit in field conditions can be explained by the temperature optimum of photosynthesis. *Agric. For. Meteorol.* **189–190**, 2–10.

Farquhar G. D., Ehleringer J. R. and Hubick K. T. (1989) Carbon isotope discrimination and photosynthesis. *Ann. Rev. Plant Physiol. Plant Mol. Biol.* **40**, 503–537.

Figge R. A. and White J. W. C. (1995) High-resolution Holocene and late glacial atmospheric CO_2 record. Variability tied to changes in thermohaline circulation. *Global Biogeochem. Cycles* **9**, 391–403.

Fletcher M.-S. and Moreno P. I. (2012) Have the Southern Westerlies changed in a zonally symmetric manner over the last 14,000 years? A hemisphere-wide take on a controversial problem. *Quatern. Int.* **253**, 32–46.

Ghashghaie J., Badeck F. W., Lanigan G., Nogués S., Tcherkez T., Deléens E., Cornic G. and Griffiths H. (2003) Carbon isotope fractionation during dark respiration and photorespiration in C_3 plants. *Phytochem. Rev.* **2**, 145–161.

Goodrich J. P., Campbell D. I., Schipper L. A., Clearwater M. J. and Rutledge S. (2015) Vapour pressure deficit is a critical climate control on GPP and the light response of NEE at a Southern Hemisphere bog. *Agric. For. Meteorol.* **203**, 54–63.

Hodges T. A. and Rapson G. L. (2010) Is *Empodisma minus* the ecosystem engineer of the FBT (fen-bog transition zone) in New Zealand? *J. Royal Soc. New Zealand* **40**, 181–207.

Holzkämper S., Tillman P. K., Kuhry P. and Esper J. (2012) Comparison of stable carbon and oxygen isotopes in *Picea glauca* tree rings and *Sphagnum fuscum* moss remains from subarctic Canada. *Quatern. Res.* **78**, 295–302.

Hong Y. T., Wang Z. G., Jiang H. B., Lin Q. H., Hong B., Zhu Y. X., Wang Y., Xu L. S., Leng X. T. and Li H. D. (2001) A 6000-year record of changes in drought and precipitation in northeastern China based on a $\delta^{13}C$ time series from peat cellulose. *Earth Planet. Sci. Lett.* **185**, 111–119.

Hong Y. T., Hong B., Lin Q. H., Zhu Y. X., Shibata Y., Hirota M., Uchida M., Leng X. T., Jiang H. B., Xu H., Wang H. and Yi L. (2003) Correlation between Indian Ocean summer monsoon and north Atlantic climate during the Holocene. *Earth Planet. Sci. Lett.* **211**, 371–380.

Hong Y. T., Hong B., Lin Q. H., Shibata Y., Hirota M., Zhu Y. X., Leng X. T., Wang Y., Wang H. and Li Y. (2005) Inverse phase oscillations between the East Asian and Indian Ocean summer monsoons during the last 12,000 years and paleo-El Niño. *Earth Planet. Sci. Lett.* **231**, 337–346.

Hong B., Hong Y. T., Lin Q. H., Shibata Y., Uchida M., Zhu Y. X., Leng X. T., Wang Y. and Cai C. C. (2010) Anti-phase oscillation of Asian monsoons during the Younger Dryas period: evidence from peat cellulose $\delta^{13}C$ of Hani, Northeast China. *Paleogeogr. Paleoclimatol. Paleoecol.* **297**, 214–222.

Kaislahti-Tillman P., Holzkämper S., Kuhry P., Sannel A. B. K., Loader N. J. and Robertson I. (2010) Stable carbon and oxygen isotopes in *Sphagnum fuscum* peat from subarctic Canada: implications for palaeoclimate studies. *Chem. Geol.* **270**, 216–226.

Kaplan J. O., Bigelow N. H., Bartlein P. J., Christensen T. R., Cramer W., Harrison S. P., Matveyeva N. V., McGuire A. D., Murray D. F., Prentice I. C., Razzhivin V. Y., Smith B., Walker D. A., Anderson P. M., Andreev A. A., Brubaker L. B., Edwards M. E. and Lozhkin A. V. (2003) Climate change and Arctic ecosystems II: Modeling, palaeodata-model comparisons and future projections. *J. Geophys. Res. Atmos.* **108**, D198171. http://dx.doi.org/10.1029/2002JD002559.

Kidson J. W. (2000) An analysis of New Zealand synoptic types and their use in defining weather regimes. *Int. J. Climatol.* **20**, 299–316.

Lamentowicz M., Cedro A., Gałka M., Goslar T., Miotk-Szpiganowicz G., Mitchell E. A. D. and Pawlyta J. (2008) Last millennium palaeoenvironmental changes from a Baltic bog (Poland) inferred from stable isotopes, pollen, plant macrofossils and testate amoebae. *Palaeogeogr. Palaeoclimatol. Palaeoecol.* **265**, 93–106.

Liu W., Feng X., Ning Y., Zhang Q., Cao Y. and An Z. (2005) $\delta^{13}C$ variation of C3 and C4 plants across an Asian monsoon rainfall gradient in arid northwestern China. *Glob. Change Biol.* **11**, 1094–1100.

Loader N. J., Robertson I., Barker A. C., Switsur V. R. and Waterhouse J. S. (1997) An improved technique for the batch processing of small wholewood samples to α-cellulose. *Chem. Geol.* **136**, 313–317.

Loader N. J., Young G. H. F., Grudd H. and McCarroll D. (2013) Stable carbon isotopes from Torneträsk, northern Sweden provide a millennial length reconstruction of summer sunshine and its relationship to Arctic circulation. *Quatern. Sci. Rev.* **62**, 97–113.

Loisel J., Garneau M. and Hélie J. F. (2009) Modern *Sphagnum* $\delta^{13}C$ signatures follow a surface moisture gradient in two boreal peat bogs, James Bay lowlands, Québec. *J. Quat. Sci.* **24**, 209–214.

Loisel J., Garneau M. and Hélie J. F. (2010) *Sphagnum* $\delta^{13}C$ values as indicators of palaeohydrological changes in a peat bog. *Holocene* **20**, 285–291.

Lorrey A., Fowler A. M. and Salinger J. (2007) Regional climate regime classification as a qualitative tool for interpreting multi-proxy palaeoclimate data spatial patterns. A New Zealand case study. *Palaeogeogr. Palaeoclimatol. Palaeoecol.* **253**, 407–433.

Ma C. M., Zhu C., Zheng C. G., Wu C. L., Guan Y., Zhao Z. P., Huang L. Y. and Huang R. (2008) High-resolution geochemistry records of climate changes since lateglacial from Dajiuhu peat in Shennongjia mountains, central China. *Chin. Sci. Bull.* **53**(Suppl. 1), 28–41.

Markel E. R., Booth R. K. and Qin Y. (2010) Testate amoebae and $\delta^{13}C$ of *Sphagnum* as surface-moisture proxies in Alaskan peatlands. *Holocene* **20**, 463–475.

McGlone M. S. (2009) Postglacial history of New Zealand wetlands and implications for their conservation. *New Zealand J. Ecol.* **33**, 1–23.

Ménot G. and Burns S. J. (2001) Carbon isotopes in ombrogenic peat bog plants as climatic indicators: calibration from an altitudinal transect in Switzerland. *Org. Geochem.* **32**, 233–245.

Ménot-Combes G., Combes P. P. and Burns S. J. (2004) Climatic information from $\delta^{13}C$ in plants by combining statistical and mechanistic approaches. *Holocene* **14**, 931–939.

Moschen R., Kuhl N., Rehberger I. and Lücke A. (2009) Stable carbon and oxygen isotopes in sub-fossil *Sphagnum*. Assessment of their applicability for palaeoclimatology. *Chem. Geol.* **259**, 262–272.

Moschen R., Kühl N., Peters S., Vos H. and Lücke A. (2011) Temperature variability at Dürres Maar, Germany during the migration period and at high medieval times, inferred from stable carbon isotopes of *Sphagnum* cellulose. *Climate Past Discuss.* **7**, 535–573.

Newnham R. M. and Lowe D. J. (2000) A fine-resolution pollen record of late glacial climate reversal from New Zealand. *Geology* **28**, 759–762.

Newnham R. M., de Lange P. J. and Lowe D. J. (1995) Holocene vegetation, climate, and history of a raised bog complex, northern New Zealand based on palynology, plant macrofossils and tephrochronology. *Holocene* **5**, 267–282.

Newnham R. N., Vandergoes M. J., Hendy C. H., Lowe D. J. and Preusser F. (2007) A terrestrial palynological record for the last two glacial cycles from southwestern New Zealand. *Quatern. Sci. Rev.* **26**, 517–535.

Nichols J., Booth R. K., Jackson S. T., Pendall E. G. and Huang Y. (2010) Differential hydrogen isotopic ratios of *Sphagnum* and vascular plant biomarkers in ombrotrophic peatlands as a quantitative proxy for precipitation—evaporation balance. *Geochim. Cosmochim. Acta* **74**, 1407–1416.

O'Leary M. H. (1981) Carbon isotope fractionation in plants. *Phytochemistry* **20**, 553–567.

Pancost R. D., Baas M., van Geel B. and Sinninghe Damste J. S. (2003) Response of an ombrotrophic bog to a regional climate event revealed by macrofossil, molecular and carbon isotopic data. *Holocene* **13**, 921–932.

Prentice I. C., Sykes M. T. and Cramer W. (1993) A simulation model for the transient effects of climate change on forest landscapes. *Ecol. Model.* **65**, 51–70.

Price G. D., McKenzie J. E., Pilcher J. R. and Hoper S. T. (1997) Carbon-isotope variation in *Sphagnum* from hummock-hollow complexes: implications for Holocene climate reconstruction. *Holocene* **7**, 229–233.

R Development Core Team (2014) *R: a language and environment for statistical computing*. R Foundation for Statistical Computing, Vienna, Austria.

Rice S. K. and Giles L. (1996) The influence of water content and leaf anatomy on carbon isotope discrimination and photosynthesis in *Sphagnum*. *Plant, Cell Environ.* **19**, 118–124.

Royles J., Ogée J., Wingate L., Hodgson D. A., Convey P. and Griffiths H. (2012) Carbon isotope evidence for recent climate-related enhancement of CO_2 assimilation and peat accumulation rates in Antarctica. *Glob. Change Biol.* **18**, 3112–3124.

Seibt U., Rajabi A., Griffiths H. and Berry J. A. (2008) Carbon isotopes and water use efficiency: sense and sensitivity. *Oecologia* **155**, 441–454.

Sekiya N. and Yano K. (2008) Stomatal density of cowpea correlates with carbon isotope discrimination in different phosphorus, water and CO_2 environments. *New Phytol.* **179**, 799–807.

Skrzypek G., Kalużny A., Wojtuń B. and Jędrysek M. O. (2007) The carbon stable isotopic composition of mosses: a record of temperature variation. *Org. Geochem.* **38**, 1770–1781.

Stebich M., Mingramb J., Moschen R., Thiele A. and Schrödere C. (2011) Comments on "Anti-phase oscillation of Asian monsoons during the Younger Dryas period: Evidence from peat cellulose $\delta^{13}C$ of Hani, Northeast China" by Hong, B., Hong, Y. T., Lin, Q. H., Shibata, Y., Uchida, M., Zhu, Y. X., Leng, X. T., Wang, Y. and Cai, C. C. [Palaeogeography, Palaeoclimatology, Palaeoecology 297 (2010) 214–222]. *Palaeogeogr. Palaeoclimatol. Palaeoecol.* **310**, 464–470.

Ummenhofer C. C. and England M. H. (2007) Interannual extremes in New Zealand precipitation linked to modes of Southern Hemisphere climate variability. *J. Clim.* **20**, 5418–5440.

Van der Knaap W. O., Lamentowicz M., van Leeuwen J. F. N., Hangartner S., Leuenberger M., Mauquoy D., Goslar T., Mitchell E. A. D., Lamentowicz L. and Kamenik C. (2011) A multi-proxy, high-resolution record of peatland development and its drivers during the last millennium from the subalpine Swiss Alps. *Quatern. Sci. Rev.* **30**, 3467–3480.

Vandergoes M. J., Newnham R. M., Preusser F., Hendy C. H., Lowell T. V., Fitzsimons S. J., Hogg A. G., Kasper H. U. and Schluechter C. (2005) Regional insolation forcing of late quaternary climate change in the Southern Hemisphere. *Nature* **436**, 242–245.

Wagstaff S. and Clarkson B. (2012) Systematics and ecology of the Australasian genus *Empodisma* (Restionaceae) and description of a new species from peatlands in northern New Zealand. *PhytoKeys* **13**, 39–79.

Wang G., Han J. and Liu T. (2003) The carbon isotope composition of C3 herbaceous plants in loess area of northern China. *Sci. China Series (Series D)* **46**, 1069–1076.

Whinam J., Hope G. S. (2005) The peatlands of the Australasian Region. In *Mires. From Siberia to Tierra del Fuego* (ed. G. M. Steiner). Stapfia 85, pp. 397–433.

White J. W. C., Ciais P., Figge R. A., Kenny R. and Markgraf V. (1994) A high-resolution record of atmospheric CO_2 content from carbon isotopes in peat. *Nature* **367**, 153–156.

Williams T. G. and Flanagan L. B. (1996) Effect of changes in water content on photosynthesis, transpiration and discrimination against $^{13}CO_2$ and $C^{18}O^{16}O$ in *Pleurozium* and Sphagnum. *Oecologia* **108**, 38–46.

Woodley E. J., Loader N. J., McCarroll D., Young G. H. F., Robertson I., Heaton T. H. E., Gagen M. H. and Warham J. O. (2012) High-temperature pyrolysis/gas chromatography/isotope ratio mass spectrometry: simultaneous measurement of the stable isotopes of oxygen and carbon in cellulose. *Rapid Commun. Mass Spectrom.* **26**, 109–114.

Xu Z. and Zhou G. (2008) Responses of leaf stomatal density to water status and its relationship with photosynthesis in a grass. *J. Exp. Bot.* **59**, 3317–3325.

Young G. H. F., Loader N. J. and McCarroll D. (2011) A large scale comparative study of stable carbon isotope ratios determined using on-line combustion and low-temperature pyrolysis techniques. *Palaeogeogr. Palaeoclimatol. Palaeoecol.* **300**, 23–28.

Young G. H. F., Bale R. J., Loader N. J., McCarroll D., Nayling N. and Vousden N. (2012) Central England temperature since AD 1850: the potential of stable carbon isotopes in British oak trees to reconstruct past summer temperatures. *J. Quat. Sci.* **27**, 606–614.

Zhang C., Chen F. and Jin M. (2003) Study on modern plant C-13 in western China and its significance. *Chin. J. Geochem.* **22**, 97–106.

Zhang J., Chen F., Holmes J. A., Li H., Guo X., Wang J., Li S., Lü Y., Zhao Y. and Qiang M. (2011) Holocene monsoon climate documented by oxygen and carbon isotopes from lake sediments and peat bogs in China: a review and synthesis. *Quatern. Sci. Rev.* **30**, 1973–1987.

Associate editor: Thomas S. Bianchi